Arch Biol Sci. 2016;68(4):767-772 DOI:10.2298/ABS150618061G

METHODS FOR STUDYING THE LOCALIZATION OF MITOCHONDRIAL COMPLEXES III AND IV BY IMMUNOFLUORESCENT AND IMMUNOGOLD MICROSCOPY

Igor Golić[1], Marija Aleksić[1], Anita Lazarević[1], Maja Bogdanović[1], Slavica Jonić[2] and Aleksandra Korać[1,*]

[1] *Center for Electron Microscopy, Faculty of Biology, University of Belgrade,* Studentski trg 16, Belgrade, Serbia

[2] *IMPMC, Sorbonne Universités – CNRS UMR 7590, UPMC Univ Paris 6, MNHN, IRD UMR 206*, 4 Place Jussieu, Paris, France

***Corresponding author:** aleksandra.korac@bio.bg.ac.rs

Received: June 18, 2015; **Revised**: March 2, 2016; **Accepted**: March 3, 2016; **Published online**: July 27, 2016

Abstract: The localization of proteins within a cell is very important for studying protein colocalization and subsequently understanding protein-protein interactions at the subcellular level. Using mitochondrial protein localization as a model, we established methods to study the localization of electron transport chain complexes (ETCCs), specifically complexes III and IV, in brown adipose tissue (BAT) and mitochondria. Immunofluorescent and immunogold techniques were applied to BAT paraffin sections and thin Araldite sections of mitochondria-enriched fractions, respectively. Microscopic analysis clearly showed mitochondrial localization of complexes III and IV, as well their colocalization. In addition, 10 and 20 nm gold particles were capable of identifying the localization of complexes within mitochondrial cristae. The methods described in this study may be a beneficial addition to currently utilized methods for accurately identifying the localization of ETCCs, their colocalization with other proteins and their distribution inside the cell and cellular compartments. Lastly, this method can also be used to study the molecular architecture of BAT mitochondria by analyzing fixed and postfixed thin plastic sections with electron microscopy (EM).

Key words: mitochondria; immunofluorescence; immunogold; localization; brown adipose tissue

INTRODUCTION

Studying the localization of different proteins and their potential for colocalization is a method commonly utilized to better understand protein-protein interactions on a subcellular level [1]. Proteins that localize in the same compartments can be studied using microscopic analysis, which uses antibodies specific to the protein of interest. Despite the efforts of several research groups, a simple and reliable technique and microscopic analysis for studying protein localization *in situ* at the subcellular level has not yet been developed.

Immunofluorescent labeling is widely used to study the localization of structures [2], specific proteins [3,4], and protein interactions at the subcellular level [5]. Fluorescent microscopy provides insight into protein localization and distribution, and can be utilized to study live cells and tissues. However, one major disadvantage associated with confocal microscopy is that the image lateral resolution is approximately 180-250 nm, which becomes narrowed using super-resolution fluorescence microscopy [6], but the image lacks the sharpness necessary to determine the protein's precise location. One specific type of immunolabeling, immunogold, can determine the precise location of a protein at ultrastructural levels, because intracellular structures can be examined at a resolution of 0.2 nm [7]. Colloidal gold particles are distinct from subcellular structures and are easily visualized, possessing a uniform shape. Immunogold labeling is primarily utilized to obtain images of the localization of subcellular structures [8-10] or specific molecules and proteins [11-13] at an ultrastructural level. One disadvantage with this method is that it is not possible to study live cells due to the technical limitations associated with the electron microscope (EM). To preserve the samples, EM requires fixation and postfixation steps that can significantly alter the antigens. To overcome this limitation, the Tokuyasu method in cryo-electron microscopy (Cryo-EM) [14] was developed. However, sample thickness remained

a limitation for examining the molecular architecture. To address this limitation, cryo-electron microscopy of vitreous sections (CEMOVIS) was introduced, which allows for thin sections of frozen samples to be studied at a higher resolution [15]. Although this procedure allows for ultrathin sections to be directly obtained from vitrified tissue samples, the mechanical force from sectioning the sample can result in noticeable artifacts [16].

To address the limitations associated with both cryo- and classical EM, mild fixatives and low-temperature resins (e.g., Lowicryl) have been tested. However, these resin-embedded sections resulted in poor morphological details, which were not acceptable for the observation of protein localization at the subcellular level [17]. In addition, low-temperature resins and several cryo-EM immunogold methods are not reliable for the study of protein localization. Regardless of this disadvantage, several resins (e.g., Araldite and LR White) are commonly used for EM due to their broad applications [18]: for the same tissue sample, results from EM analysis of resin-embedded sections strongly correlate with the results observed from light microscopy analysis of semi-thin sections [19].

Brown adipose tissue (BAT) is rich in mitochondria due to its specific physiological role in non-shivering thermogenesis [20]. BAT mitochondria have well-developed, lamellar and parallel organized cristae [21, 22]. Mitochondria are dispersed throughout brown adipocyte cytoplasm with greater density observed in close proximity to lipid droplets. Upon β-adrenergic activation of brown adipocytes, hormone-sensitive lipase releases fatty acids from the lipid droplet as substrates for the mitochondrial production of heat via uncoupling protein 1 (UCP1) [20].

Understanding the localization of mitochondrial proteins and complexes *in situ* may provide more insight into their role in cell bioenergetics and death. However, convenient and reliable methods to study these systems have not yet been developed. In light of this, the goal of this study was to develop a simple and reliable method for microscopically analyzing protein localization at a subcellular level. Specifically, we were interested in studying proteins within the mitochondrial complexes III and IV at various cell levels (e.g., tissue and mitochondria-enriched cell fractions). To accomplish this, we used sequential immunofluorescent and immunogold analyses to determine the localization of complex III and IV proteins.

MATERIALS AND METHODS

Experimental design

All procedures performed in this study were approved by the Ethics Committee for the Treatment of Experimental Animals (Faculty of Biology, University of Belgrade, Serbia). Experiments were performed utilizing two-month-old male Wistar rats (190-260 g), maintained at 22±1°C, in 12-h light/dark cycles, and with *ad libitum* access to water and standard pelleted food. Control rats (n=6) received an intraperitoneal injection of 0.9% saline (1 ml/kg) on day one. Three hours after the last injection, animals were killed using a decapitator (Harvard Apparatus, USA). The interscapular portion of BAT was dissected out and the left portion was analyzed via confocal microscopy.

Isolation of BAT mitochondria-enriched fractions

BAT mitochondria-enriched fractions were isolated according to a previously published protocol [23,24], with minor modifications. Briefly, the BAT was minced with fine scissors, homogenized using a glass Potter-Elvehjem homogenizer with a Teflon pestle and filtered through two layers of surgical gauze. During isolation, all tissues were stored in 0-4°C. Homogenates were centrifuged at 8500xg for 10 min at 4°C in a Beckman Optima L-100 XP ultracentrifuge. After the first centrifugation, the supernatant and fat layer were discarded. Pellets were resuspended in ice-cold 250 mM sucrose medium, transferred to a clean tube, and centrifuged at 800xg for 10 min. Supernatants were collected and centrifuged at 8500xg for 10 min. The resulting pellet was suspended in 250 mM sucrose medium with 1% ethylenediaminetetraacetic acid (EDTA) and 0.6% fatty-acid-free bovine serum albumin (BSA), and centrifuged at 8500xg for 10 min.

Aliquots of freshly isolated mitochondria-enriched fractions were fixed with 2.5% glutaraldehyde (v/v) in 0.1 M Sørensen phosphate buffer (PB; pH 7.2) and centrifuged at 14000xg for 10 min. The resulting

pellets were washed in PB, postfixed in 2% osmium tetroxide in PB, dehydrated using increasing concentrations of ethanol and embedded in Araldite (Fluka, Germany). Ultrathin sections of isolated mitochondria were obtained using a Leica UC6 ultramicrotome (Leica Microsystems, Germany) mounted on nickel grids, and prepared for immunogold analyses.

Immunogold localization of mitochondrial complexes

To identify the localization of complexes III and IV for each mitochondrion, we used immunogold analysis. After antigen retrieval in citrate buffer and blocking with 5% BSA in Tris-buffered saline, 0.1% Tween 20 (TBST), grids were incubated overnight in 4°C with the primary antibody raised against complex III (1:100, ab14745; Abcam, UK). After rinsing in TBST, the grids were incubated with 10 nm gold-labeled secondary antibody (1:20, ab27241; Abcam). Saturated dilutions of the secondary antibody provided complete binding for all available antigens on the primary antibody. Next, the grids were washed 10 times in TBST, blocked with 5% BSA and incubated with the primary antibody raised against complex IV (1:100, ab14744; Abcam) overnight at 4°C. Following a TBST rinse, the grids were incubated with 20 nm gold-labeled secondary antibody (1:20, ab27242; Abcam). After washing in TBST and double distilled water, the grids were air-dried. The specificity of the immunogold analyses was performed using single gold-labeled samples (e.g., samples incubated with anti-CIII or anti-CIV antibodies and their respective secondary antibodies). Specificity was further verified by including parallel negative controls. Negative controls consisted of the following reagents: (i) 10 nm gold secondary antibody, (ii) 20 nm gold secondary antibody, (iii) primary antibody against CIII, 10 nm gold secondary antibody, and later 20 nm gold secondary antibody, (iv) primary antibody against CIV, 20 nm gold secondary antibody, and later 10 nm gold secondary antibody.

Transmission electron microscopy of isolated mitochondria

Interscapular BAT was pooled from six rats, placed in ice-cold 250 mM sucrose medium, freed of white fat and connective tissue, and the mitochondria-enriched fraction was isolated. Sections were examined with a Philips CM12 transmission electron microscope (Philips/FEI, The Netherlands) equipped with the digital camera SIS MegaView III (Olympus Soft Imaging Solutions, Germany).

Immunofluorescence

Immediately after dissection, one portion of the BAT was fixed in 4% paraformaldehyde in 0.1 M phosphate buffered saline (PBS) overnight at 4°C and processed for paraffin embedding. For immunofluorescence analysis, 7-μm-thick paraffin-embedded BAT sections were deparaffinized and rehydrated.

To analyze the colocalization of complexes III and IV, we performed sequential immunofluorescence. Briefly, after antigen retrieval in citrate buffer and blocking with 10% normal goat serum and 1% BSA, sections were incubated with the primary antibody raised against the UQCRC2 for complex III (1:100, ab14745; Abcam) overnight at 4°C. After rinsing in TBST, sections were labeled with Alexa Fluor 488 secondary antibody (1:400, A-11029; Life Technologies, USA). The slides were then washed three times in TBST, blocked with 10% normal goat serum and 1% BSA, and incubated with the primary antibody raised against cytochrome *c* oxidase or complex IV (1:100, ab14744; Abcam) overnight at 4°C. After rinsing in TBST, sections were incubated with Alexa Fluor 633 secondary antibody (1:400, A-21052; Life Technologies) and washed again in TBST prior to counterstaining with nuclear stain SYTOX Orange (1:1000) for 5 min. After this final step, the slides were washed in TBS and mounted with Mowiol.

Confocal images were obtained using a Leica TCS SP5 II confocal microscope (Leica Microsystems) in sequential mode to avoid crosstalk between channels. After verification of single-labeled sections, double-labeled sections were excited with 488 and 633 nm lasers, respectively. Nuclei were visualized using a 543 nm laser, and blue false-colored for the clear distinction of green/red channels. Immunofluorescence specificity was tested by running parallel negative controls. The negative controls consisted of the following conditions: i) Alexa Fluor 488 secondary antibody, ii) Alexa Fluor 633 secondary antibody, iii) a mixture of

Alexa Fluor 488 and 633 secondary antibodies, iv) primary antibody against CIII, Alexa Fluor 488 secondary antibody, and later Alexa Fluor 633 secondary antibody, v) primary antibody against CIV, Alexa Fluor 633 secondary antibody, and later Alexa 488 secondary antibody.

RESULTS AND DISCUSSION

Immunofluorescent analysis of mitochondrial complexes

To study metabolic processes (or thermogenesis) in mitochondria, it is important to understand the localization of proteins and their interactions at the subcellular and cellular level. Confocal microscopy can be used to identify the location of a protein and subsequently draw conclusions about their subcellular interactions. However, to fully understand protein-protein interactions, it is necessary to view cells on a nanoscale level using EM [25].

In this study, we used confocal microscopy to analyze the localization of complexes III and IV in brown adipocytes. Our results clearly showed their colocalization within the mitochondria (Fig. 1), which is in accordance with previously published studies [26-29]. It is also possible to calculate the colocalization rate or Pearson's correlation coefficient between two proteins of interest using confocal microscope manufacturer's software [30,31].

Immunogold analysis of mitochondrial complexes

In addition to the immunofluorescence analysis, an immunogold procedure was used to identify the precise location of complexes within mitochondria-enriched fractions at an ultrastructural level (Fig. 2). It is important to note that some complexes may not have been recognized by the primary antibody because they were blocked by other antigen-antibody complexes. At the ultrastructural level, we observed the localization of the specific complexes within the mitochondrial cristae (Fig. 2), which provides evidence for their involvement in supercomplex organization [32-35]. Using ImageJ software (NIH, USA), immunogold particles can be counted to calculate the ratio of examined proteins and their spatial distributions [36-38]. Current hypotheses suggest that the morphology/topology of the inner mitochondrial membrane is strongly related to biochemical function, energy state and the pathophysiological state of the mitochondria [39]. Although tremendous improvements have been made to EM methodologies, no standard procedure has been published for the study of the localization of proteins at the subcellular level.

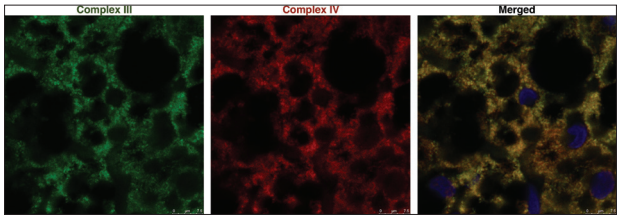

Fig. 1. Immunofluorescence of complexes III and IV in BAT. Double labeling with antibodies raised against complexes III (green) and IV (red). Nuclei were stained with SYTOX Orange (blue). Scale bar: 7.5 μm. BAT – brown adipose tissue.

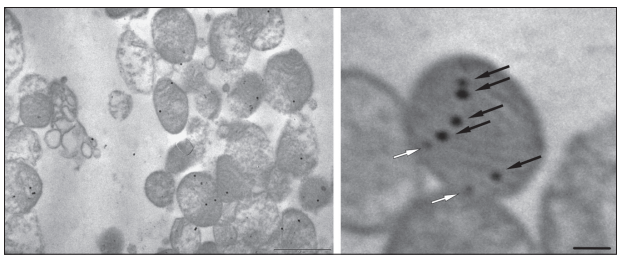

Fig. 2. Immunogold localization of complexes III (10 nm gold) and IV (20 nm gold) in BAT mitochondria-enriched fractions. **A** – Mitochondria-enriched fraction and **B** – immunogold localization of complexes III (10 nm gold, white arrows) and IV (20 nm gold, black arrows) within mitochondrial cristae. Scale bar: 1 μm (**A**); 100 nm (**B**). BAT – brown adipose tissue.

Taking into account the advantages and disadvantages associated with immunofluorescent and immunogold labeling, we described a method to study the colocalization of ETCCs (complexes III and IV) in BAT mitochondria. Our method consisted of an immunogold procedure that used EM-standard fixed tissues embedded in Araldite resin, which resulted in a rapid, inexpensive, efficient and reliable method for studying protein localization, colocalization and/or spatial distribution. Based on our results, we recommend the use of this method in the study of colocalization and the relationship between proteins in brown adipocyte mitochondria.

Acknowledgments: This work was financially supported by the Ministry of Education, Science and Technological Development of the Republic of Serbia, Research Grants 173054 and 173055.

Authors' contribution: IG and AK conceived and designed the experiments. IG, MA, AL, MB and AK performed the experiments. IG, MA, AL, MB, SJ and AK analyzed the data. SJ and AK contributed reagents/materials/analysis tools. IG and AK wrote the paper.

Conflict of interest disclosure: The authors declare that they have no conflict of interest.

REFERENCES

1. Barzda V, Greenhalgh C, Aus der Au J, Elmore S, van Beek J, Squier J. Visualization of mitochondria in cardiomyocytes by simultaneous harmonic generation and fluorescence microscopy. Opt Express. 2005;13(20):8263-76.
2. Zhao X, He Y, Gao J, Fan L, Li Z, Yang G, Chen H. Caveolin-1 expression level in cancer associated fibroblasts predicts outcome in gastric cancer. PLoS One. 2013;8(3):e59102.
3. Gronemeyer T, Wiese S, Grinhagens S, Schollenberger L, Satyagraha A, Huber LA, et al. Localization of Rab proteins to peroxisomes: a proteomics and immunofluorescence study. FEBS Lett. 2013;587(4):328-38.
4. Vitha S, Osteryoung KW. Immunofluorescence microscopy for localization of Arabidopsis chloroplast proteins. Methods Mol Biol. 2011;774:33-58.
5. Manczak M, Reddy PH. Abnormal interaction of VDAC1 with amyloid beta and phosphorylated tau causes mitochondrial dysfunction in Alzheimer's disease. Hum Mol Genet. 2012;21(23):5131-46.
6. Schermelleh L, Heintzmann R, Leonhardt H. A guide to super-resolution fluorescence microscopy. J Cell Biol. 2010;190(2):165-75.
7. Spence JCH. High-resolution electron microscopy. 4th ed. Oxford: Oxford University Press; 2013. 406 p.
8. Bergersen L, Rafiki A, Ottersen OP. Immunogold cytochemistry identifies specialized membrane domains for monocarboxylate transport in the central nervous system. Neurochem Res. 2002;27(1-2):89-96.
9. Hamzei-Sichani F, Kamasawa N, Janssen WG, Yasumura T, Davidson KG, Hof PR, Wearne SL, Stewart MG, Young SR, Whittington MA, Rash JE, Traub RD. Gap junctions on hippocampal mossy fiber axons demonstrated by thin-section electron microscopy and freeze fracture replica immunogold labeling. P Natl Acad Sci USA. 2007;104(30):12548-53.
10. Nielsen S, Nagelhus EA, Amiry-Moghaddam M, Bourque C, Agre P, Ottersen OP. Specialized membrane domains for water transport in glial cells: high-resolution immunogold cytochemistry of aquaporin-4 in rat brain. J Neurosci. 1997;17(1):171-80.
11. Rash JE, Staines WA, Yasumura T, Patel D, Furman CS, Stelmack GL, Nagy JI. Immunogold evidence that neuronal gap junctions in adult rat brain and spinal cord contain connexin-36 but not connexin-32 or connexin-43. P Natl Acad Sci USA. 2000;97(13):7573-8.
12. Sinha AA, Jamuar MP, Wilson MJ, Rozhin J, Sloane BF. Plasma membrane association of cathepsin B in human prostate cancer: biochemical and immunogold electron microscopic analysis. Prostate. 2001;49(3):172-84.
13. Vielhaber G, Pfeiffer S, Brade L, Lindner B, Goldmann T, Vollmer E, Hintze U, Wittern KP, Wepf R. Localization of ceramide and glucosylceramide in human epidermis by immunogold electron microscopy. J Invest Dermatol. 2001;117(5):1126-36.
14. Tokuyasu KT. A technique for ultracryotomy of cell suspensions and tissues. J Cell Biol. 1973;57(2):551-65.
15. Studer D, Humbel BM, Chiquet M. Electron microscopy of high pressure frozen samples: bridging the gap between cellular ultrastructure and atomic resolution. Histochem Cell Biol. 2008;130(5):877-89.
16. Al-Amoudi A, Studer D, Dubochet J. Cutting artefacts and cutting process in vitreous sections for cryo-electron microscopy. J Struct Biol. 2005;150(1):109-21.
17. De Paul AL, Torres AI, Quintar AA, Maldonado CA, Mukdsi JH, Petiti JP, Gutiérrez S. Immunoelectron microscopy: a reliable tool for the analysis of cellular processes. In: Denghani H, editor. Applications of Immunocytochemistry. Rijeka: INTECH Open Access Publisher; 2012. 65-96.
18. Skepper JN, Powell JM. Immunogold staining of epoxy resin sections for transmission electron microscopy (TEM). CSH Protoc. 2008;2008(6):pdbprot5015.
19. Koga D, Kusumi S, Shodo R, Dan Y, Ushiki T. High-resolution imaging by scanning electron microscopy of semithin sections in correlation with light microscopy. Microscopy. 2015;64(6):387-94.
20. Cannon B, Nedergaard J. Brown adipose tissue: function and physiological significance. Physiol Rev. 2004;84(1):277-359.
21. Perkins GA, Frey TG. Recent structural insight into mitochondria gained by microscopy. Micron. 2000;31(1):97-111.
22. Rodriguez-Cuenca S, Pujol E, Justo R, Frontera M, Oliver J, Gianotti M, Roca P. Sex-dependent thermogenesis, differences in mitochondrial morphology and function, and adrenergic response in brown adipose tissue. J Biol Chem. 2002;277(45):42958-63.
23. Cannon B, Lindberg O. Mitochondria from brown adipose tissue: isolation and properties. Method Enzymol. 1979;55:65-78.
24. Cannon B, Nedergaard J. Studies of thermogenesis and mitochondrial function in adipose tissues. Methods Mol Biol. 2008;456:109-21.
25. Dudkina NV, Kouril R, Bultema JB, Boekema EJ. Imaging of organelles by electron microscopy reveals protein-protein interactions in mitochondria and chloroplasts. FEBS Lett. 2010;584(12):2510-5.
26. Carr HS, Winge DR. Assembly of cytochrome c oxidase within the mitochondrion. Acc Chem Res. 2003;36(5):309-16.
27. Han D, Williams E, Cadenas E. Mitochondrial respiratory chain-dependent generation of superoxide anion and its release into the intermembrane space. Biochemical J. 2001;353(Pt 2):411-6.
28. Herrmann JM, Funes S. Biogenesis of cytochrome oxidase-sophisticated assembly lines in the mitochondrial inner membrane. Gene. 2005;354:43-52.

29. Schilling B, Murray J, Yoo CB, Row RH, Cusack MP, Capaldi RA, Gibson BW. Proteomic analysis of succinate dehydrogenase and ubiquinol-cytochrome c reductase (Complex II and III) isolated by immunoprecipitation from bovine and mouse heart mitochondria. Biochim Biophys Acta. 2006;1762(2):213-22.
30. Lu W, Man H, Ju W, Trimble WS, MacDonald JF, Wang YT. Activation of synaptic NMDA receptors induces membrane insertion of new AMPA receptors and LTP in cultured hippocampal neurons. Neuron. 2001;29(1):243-54.
31. Zinchuk V, Grossenbacher-Zinchuk O. Quantitative colocalization analysis of fluorescence microscopy images. Curr Protoc Cell Biol. 2014;62: 4.19.1-4.19.14.
32. Dudkina NV, Kouril R, Peters K, Braun HP, Boekema EJ. Structure and function of mitochondrial supercomplexes. Biochim Biophys Acta. 2010;1797(6-7):664-70.
33. Vonck J, Schafer E. Supramolecular organization of protein complexes in the mitochondrial inner membrane. Biochim Biophys Acta. 2009;1793(1):117-24.
34. Suthammarak W, Morgan PG, Sedensky MM. Mutations in mitochondrial complex III uniquely affect complex I in Caenorhabditis elegans. J Biol Chem. 2010;285(52):40724-31.
35. Schagger H, Pfeiffer K. Supercomplexes in the respiratory chains of yeast and mammalian mitochondria. EMBO J. 2000;19(8):1777-83.
36. Bergersen LH, Storm-Mathisen J, Gundersen V. Immunogold quantification of amino acids and proteins in complex subcellular compartments. Nat Protoc. 2008;3(1):144-52.
37. Philimonenko AA, Janacek J, Hozak P. Statistical evaluation of colocalization patterns in immunogold labeling experiments. J Struct Biol. 2000;132(3):201-10.
38. Chen Q, Mahendrasingam S, Tickle JA, Hackney CM, Furness DN, Fettiplace R. The development, distribution and density of the plasma membrane calcium ATPase 2 calcium pump in rat cochlear hair cells. Eur J Neurosci. 2012;36(3):2302-10.
39. Mannella CA, Lederer WJ, Jafri MS. The connection between inner membrane topology and mitochondrial function. J Mol Cell Cardiol. 2013;62:51-7.